PLOS Climate

RESEARCH ARTICLE

Modeling snowmelt-driven streamflow dynamics in a Himalayan Basin under climate warming scenarios

Romana Jamshed[1], **Esha Naeem**[1], **Adnan Ahmad Tahir**[1*], **Muhammad Irshad**[1], **Faizan-ur-Rehman Qaisar**[2], **Awais Arifeen**[1], **Sher Muhammad**[3*], **Wu Kunpeng**[4], **Muhammad Abrar Faiz**[5]

1 Department of Environmental Sciences, COMSATS University Islamabad (CUI), Abbottabad Campus, Abbottabad, Pakistan, **2** Department of Earth Sciences, COMSATS University Islamabad (CUI), Abbottabad Campus, Abbottabad, Pakistan, **3** International Center for Integrated Mountain Development (ICIMOD), Kathmandu, Nepal, **4** Institute of International Rivers and Eco-Security, Yunnan University, Kunming, China, **5** School of Water Conservancy & Civil Engineering, Northeast Agricultural University, Harbin, China

* adnantahir@cuiatd.edu.pk (AAT); Sher.Muhammad@icimod.org (SM)

Citation: Jamshed R, Naeem E, Tahir AA, Irshad M, Qaisar F-u-R, Arifeen A, et al. (2025) Modeling snowmelt-driven streamflow dynamics in a Himalayan Basin under climate warming scenarios. PLOS Clim 4(10): e0000739. https://doi.org/10.1371/journal.pclm.0000739

Editor: Samuel Jonson Sutanto, Wageningen University & Research, NETHERLANDS, KINGDOM OF THE

Received: July 29, 2025

Accepted: October 8, 2025

Published: October 22, 2025

Data availability statement: All relevant data are provided in the supplementary material with a checklist of figures and tables numbers for which data is provided. The datasets used for the analyses in Figures 8–10 (daily discharge),

Abstract

The snow and glacier-fed Swat River Basin (SRB), located in the Hindukush region of Pakistan, plays a vital role in supporting ecosystems and downstream communities. However, the basin is highly vulnerable to climate change, as evidenced by frequent historical floods. This study simulated historical and future snowmelt runoff using the Snowmelt Runoff Model (SRM), integrated with an enhanced MODIS snow and glacier product (MOYDGL06*), along with Digital Elevation Model (DEM) and hydro-meteorological data. The model was calibrated and validated over 2005–2009 and 2011–2015, respectively, using basin-wide and zone-wise simulation approach. The key findings of the study indicated: 1) SRM coupled with the improved snow product effectively simulated daily river discharge, achieving mean Nash–Sutcliffe Efficiency (NSE) values of 0.90–0.91 and Volume Differences (D_v) of 0.51% to –1.31% during calibration, and NSE of 0.84–0.87 with D_v of –0.83% to –2.27% during validation. The basin-wide approach performed more consistently due to integrated hydrological representation and lower parameter uncertainty. 2) Future projections under three RCP scenarios indicate increases of ~8–18% (2046–2065) and ~7–34% (2081–2100) in mean annual flow and increases of ~7–16% and ~7–30% in mean summer flow, respectively. An increase of 1 °C in temperature is projected to enhance both seasonal and annual flows by about 6–7%. These projected increases are primarily attributed to enhanced snow and glacier melt due to rising temperatures. The findings emphasize the need for adaptive strategies in water resources management and flood risk mitigation in the study area, especially under changing climatic conditions.

as well as the daily temperature and precipitation data employed in the snowmelt-runoff model, cannot be made publicly available due to restrictions imposed by the data providers. These datasets may, however, be obtained upon formal written request from the Project Director, Surface Water Hydrology Project (SWHP), Water and Power Development Authority (WAPDA), Lahore office or by contacting via Phone#+92-42-99202211 or Email: webinfo@wapda.gov.pk, and the Deputy Director, Pakistan Meteorological Department (PMD), Islamabad, Phone#+92-51-9250367 or Email: info.cdpc@pmd.gov.pk.

Funding: This work was supported by the following funding sources: 1) the Joint Scientific Exchange Program of the Pakistan Science Foundation (PSF) and the National Natural Science Foundation of China, NSFC (Project No: PSF-NSFC/JSEP/ENV/C-COMSATS/03) received by W.K and A.A.T. 2) COMSATS Research Grant Program, CRGP (Project No: 16-05/CRGP/CUI/ATD/24) received by A.A.T and R.J. Note: The funders had no role in study design, data collection and analysis, decision to publish, or preparation of the manuscript. In addition, none of the authors received any salary from any of funders.

Competing interests: I have read the journal's policy, and the authors of this manuscript have the following competing interests: Dr. Sher Muhammad (one of the co-authors) is an Academic Editor in "PLOS Climate". The other authors have declared that no competing interests exist.

1. Introduction

The Indus River Basin (IRB) relies heavily on snow and glacial melt from the Hindukush-Karakoram-Himalaya (HKH) region [1], which accommodates the active hydrological zone of the basin [2]. The water from the Indus River is crucial for electricity generation, irrigation, and provides clean drinking water to downstream communities in Pakistan [3]. The catchment hydrology of IRB and its sub-basins in Pakistan is disrupted because the HKH region is facing significant threats from global warming and climate change resulting into enhanced glacier melting and altering snow patterns, affecting the seasonal flow of the Indus River and its tributaries [4,5]. Winter precipitation due to low pressure western weather systems is expected to escalate in the HKH region due to climate change, which is anticipated to maintain positive snow/glacier mass balance [4,6]. However, the increasing summer temperatures and monsoon precipitation will speed-up the snow and glacier melt process resulting into extreme floods in the region including Kabul and Swat River Basins [7]. Hence, Pakistan becomes one of the most vulnerable countries due to its susceptibility to the consequences of climate change. This poses a serious risk to water availability for irrigation, hydropower, and domestic use in the region and requires water resource and disaster management [8].

Swat and Kabul River catchments are frequently prone to floods such as that of 2010 with ~11327 m^3/s, impacting the 24 districts [9] of Khyber Pakhtunkhwa (KP) province of Pakistan. The surrounding areas of the districts Peshawar, Nowshera and Charsada received 200–280 mm rainfall during the 2010 flood period and became endangered to flood risks due to very high flood stage (with a discharge of ~6258 m^3/s) in the Kabul River. These areas are prone to flash as well as riverine floods [10]. District Swat's precipitation is reported to decline by -0.73 mm while temperature has risen by 0.028 °C per year during 1985–2015 period [11]. Such high temperature in high-altitude sub-catchment of IRB results in higher summer runoff due to snow and glacier melt [12] and contributes to enhance the flood frequency and magnitude and related destruction when combined with monsoon precipitation [10].

With this challenge, it is crucial to use reliable hydrological tools to simulate consequential runoff to determine the availability of water supply for future needs and mitigate the related flood hazards [2,4,5,13]. Predicting future runoff from high-altitude snow and glacier catchments through hydrological modeling (HMs) is challenging due to data limitations [14]. Various hydrological models, often combining remote sensing and ground observations, are used to simulate and forecast melt runoff in mountainous areas [2,3]. The input data for various HMs includes climatic data, drainage area, vegetation cover, soil moisture, and aquifers characteristics of the watershed to simulate the runoff [15]. Based upon spatial distribution characteristics of model, the snow melt models can be categorized as lumped, semi-distributed and distributed models [16]. The lumped snowmelt model assumes snow cover and melting rate as consistent factors across the watershed or sub-basin [17]. Semi-distributed models, including HBV [18], SWAT [13] and the Precipitation-Runoff Modeling System (PRMS) [19], usually divide the watershed into sub-watersheds or hydrological response units [20]

according to a certain characteristic of the watershed (e.g., elevation, vegetation coverage, land use types, and topographic factors) [21].

Snowmelt Runoff Model (SRM), a degree-day, lumped and conceptual model, developed by Martinec [14] is widely used for snow-fed mountainous catchments [22] which uses remotely sensed snow-cover data as basic input. By analyzing the effects of climatic variation on snowmelt flow in the Upper Indus Basin, SRM can estimate snowmelt runoff efficiently in high mountain locations. Butt and Bilal [23] endorsed that SRM in conjunction with MODIS snow cover product can be used effectively for runoff forecasts in the Astore River basin. SRM was used to efficiently simulate streamflow from snowmelt in the Buha watershed within the Qinghai Lake basin for 2003–2009 period [24]. The model performance was examined by using two different precipitation products as inputs, i.e., station measured precipitation and gridded APHRODITE-precipitation [25], with two different snow cover products, namely, flexible multiday combined MODIS Terra–Aqua (MODISMC) maps, and the standard MODIS/Terra 8-day composite (MOD10A2) product. The results of a study [26] indicated that SRM has efficiently simulated the flow in Shyok River for 2000–2006 period. The study concluded that SRM equipped with remotely sensed snow cover data is an appropriate tool to estimate snowmelt runoff in high mountain data-scarce catchments. SRM was employed to evaluate the snowmelt impacts on high flows from Ajichai catchment in northwestern Iran and found it effective to be used for high-altitude catchments [27]. All mentioned studies suggested that while selecting a snowmelt runoff simulation model, it's crucial to comprehensively consider data availability, watershed characteristics, and time scale of simulation.

The snow and glacier-fed Swat River Basin (SRB) currently lacks a comprehensive spatiotemporal assessment of its water availability. Particularly, there is a critical gap in understanding both its historical patterns and how future climate change scenarios will impact its river flow [28]. Additionally, estimating snow- and glacier-melt runoff in the field and predicting the resulting high river discharges, particularly during summer, is challenging due to limited gauging infrastructure in the SRB. This missing knowledge and data scarcity hinders effective water resource planning, hazard mitigation and adaptation strategies in this flood prone mountainous region. So, this study aimed to simulate river runoff in the SRB by coupling ground and remote sensing data with hydrological models and to estimate the future stream flow under potential climatic scenarios from the "Swat River". Specific objectives of this study are to (i) simulate the water availability in the Swat River Basin using SRM integrated with remotely sensed improved MODIS snow products, and (ii) project future river flow from SRB under various climate change scenarios for assisting the informed adaptation strategies for water resource management.

2. Hydro-geographical setting

The chosen study area, i.e., Swat River Basin (SRB), lying between 34°33′49″ and 35°54′8″ North Latitude and 71°55′8″and 72°50′38″ East Longitude, is a sub-catchment of the Indus River basin, situated in Khyber Pakhtunkhwa (KP) province of Pakistan and surrounded by Hindukush Mountain range [29]. The Swat River Basin is best described as a snow- and glacier-fed, with supplementary rain-fed contributions, particularly during the spring (February-April) and summer monsoon (June-August) period. The Swat River originates in Kalam, where two glacier-fed streams, Gabral and Ushu, converge. A mean snowmelt runoff contribution of ~65–75% is reported to the total annual runoff of the Swat River [30]. The important features of the SRB including location map, with digital elevation model (DEM), zonal classification, location of flow gauge and meteorological stations are presented in Fig 1 and Table 1. The total area of this watershed has been estimated ~5745 km^2 and has an elevation range of 681–5898 meters above mean sea level (m ASL) with mean elevation of ~2600 m ASL as estimated from the DEM and the hypsometric curve (Fig 1 and S1 Fig). Total glacier cover is estimated as ~203 km^2 (~3.5%) from the Randolf Glacier Inventory (RGI) version 7 [31]. For the application of zone-wise SRM, the SRB was divided into four zones described as A, B, C and D, classified using the elevation range as shown in Fig 1, S1 Fig and Table 1. The spatial characteristics of basin and respective zones are presented in Fig 1 and Table 1. Four weather stations (WS) Kalam, Malam Jabba, Saidu sharif, and Dir are situated inside or just outside the boundary

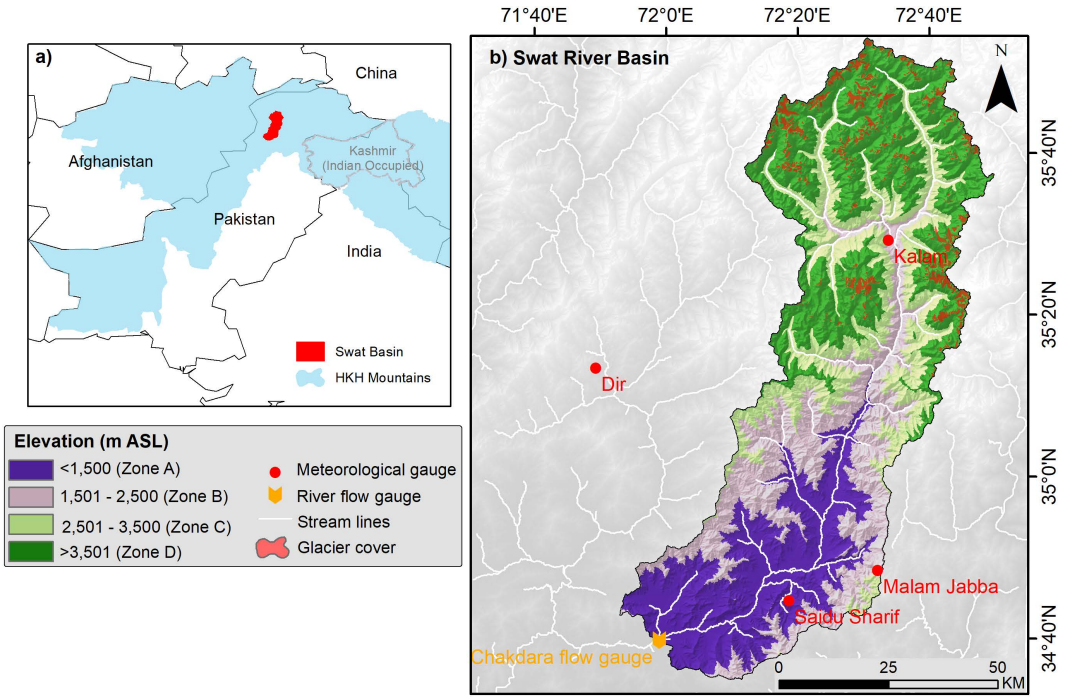

Fig 1. Study area map of the Swat River Basin. a) Location of Swat River Basin in Pakistan and HKH, and b) Digital elevation model (DEM) of Swat River Basin showing the elevation variation and superimposed by hydro-meteorological stations, streamlines and glacier cover. HKH boundary was downloaded from Regional Dataset System (RDS) portal [32] of ICIMOD. Country Shapefile was downloaded from open access Natural Earth data portal (Made with Natural Earth. Free vector and raster mapdata@naturalearthdata.com).

https://doi.org/10.1371/journal.pclm.0000739.g001

Table 1. Basin-wide and zone-wise spatial characteristics of Swat River Basin estimated from DEM for SRM application.

Zone	Area (km²)	Area (%)	Elevation band (m ASL)	Mean Elevation (m ASL)
A	1377.02	23.97	681-1500	~1150
B	1319.10	22.96	1501-2500	~1950
C	1108.00	19.28	2501-3500	~3000
D	1941.34	33.79	3501-5898	~4100
Entire Basin	~5745.45	–	681-5898	~2600

https://doi.org/10.1371/journal.pclm.0000739.t001

(Fig 1) of SRB whose data were used in this study. While the discharge data of river flow gauge installed at the Chakdara town (Fig 1) on the river bridge is used to carry out the flow simulation using SRM.

Swat valley, having a 2.3 million population, is characterized by humid, sub-humid and semi-arid climate [33]. Its maximum area is used for agriculture, while 26% is covered by wild vegetation, forests, water streams and just 4% is built-up area [34]. SRB is vulnerable to frequently occurring flood hazards and deadliest disaster, where the upper reaches of the basin experiences flash floods characteristics while intense and frequent riverine flood dominates the downstream areas due to unusual and prolonged summer monsoon rainfall as well as heavy snow and glacier melting [29,35]. Since 2000 and particularly the year 2010 and 2022, SRB has experienced the most devastating floods resulting into socio-economic and environmental losses, where agriculture, tourism, transportation and public property are found to be the most affected sectors [8]. Therefore, it becomes quite necessary to forecast the hydrology of the Swat River Basin to timely adapt to any future catastrophes that might occur in the region.

3. Data sets and methodology

This section presents data sets, sources, data treatment, methods and techniques used to achieve the objectives of this study.

3.1. Data sets, sources and treatment

To achieve the objectives of the study, two types of datasets were utilized (i) in-situ daily hydro-meteorological data, including river flow, temperature and precipitation data, and (ii) satellite based remote sensing data for elevation and daily snow cover area (SCA).

3.1.1. In-situ daily hydro-meteorological data. In-situ daily flow data as well as data of climatic variables like temperature (maximum, minimum and average) and precipitation, was obtained for the period of 10 years 2005–2015 (excluding the incomplete data of 2010) for the study area. Daily flow data of the Swat River measured at the Chakdara gauging station (Fig 1) was acquired from the "Surface Water Hydrology Project (SWHP)" of "Water and Power Development Authority (WAPDA)" while "Pakistan Meteorological Department (PMD)" provided data on climatic variables. The climatic data is measured at three stations, i.e., Saidu Sharif, Kalam and Malam Jabba located inside the SRB (Fig 1). Due to the unavailability of daily meteorological data from Kalam and Malam Jabba stations, this study relied on daily data from Saidu Sharif and a neighboring station Dir (Fig 1) for hydrological modelling. Table 2 presents the information related to flow gauge and meteorological stations used in this study for the period 2005–2015. Flow gauge data for 2010 from August-October was missing because the gauge went non-functional after 2010 floods. Therefore, this year was excluded from SRM simulations.

It is important to estimate the daily zonal temperatures for the zone-wise approach of SRM. The daily zonal mean temperatures for each of the four zones were calculated by extrapolating the mean temperature at Dir and Saidu Sharif stations and using the catchment's lapse rate value of 0.66 °C per 100 meters, which is the average of lapse rates between the weather stations as given in Table 3. The highest lapse rate (0.87 °C/100m) is found between Dir and Saidu Sharif weather stations, while lowest lapse rate (0.45 °C/100m) is between Dir and Malam Jabba. These lapse rate values were

Table 2. Information related to flow gauge and meteorological stations used in this study for the period 2005–2015.

Stations		Geographical Coordinates (Degree, Minutes, Seconds)	Elevation (m ASL)	Available Data Time Step
Flow Guage	**Chakdara**	34° 38' 38.4" N, 72° 1' 44.4" E	686	Daily
Weather Stations	Saidu Sharif	34° 43' 58.8" N, 72° 21' 0" E	961	Daily
	Dir	35° 12' 0" N, 71° 51' 0" E	1375	Daily
	Kalam	35° 28' 48" N, 72° 34' 37.2" E	2103	Monthly
	Malam Jabba	34° 48' 0" N, 2° 34' 12" E	2591	Monthly

https://doi.org/10.1371/journal.pclm.0000739.t002

Table 3. Temperature lapse rates between weather stations calculated from the available temperature data of all weather stations in the Swat River Basin.

Weather Stations (elevation, m ASL)	Lapse Rate (°C/100 meter)
Dir (1375) & Saidu Sharif (961)	0.84
Dir (1375) & Kalam (2103)	0.69
Dir (1375) & Malam Jabba (2591)	0.45
Saidu Sharif (961) & Kalam (2103)	0.75
Saidu Sharif (961) & Malam Jabba (2591)	0.55
Catchment's average lapse rate	0.66

https://doi.org/10.1371/journal.pclm.0000739.t003

calculated by using the average of available observed temperature data on two climate stations, i.e., Dir and Saidu Sharif obtained from PMD, and their elevations [36]. Actual lapse rate was crucial to obtain and use instead of global lapse rate since SRM is sensitive to change in temperature and varying snow cover data over the study period [3]. The average of the daily total precipitation recorded at Dir and Saidu Sharif weather stations was used for all the zones in basin-wide and zone-wise application of SRM although this may underrepresent the orographic precipitation and snowfall processes at higher elevations. However, SRM is designed to be used for data scarce mountainous areas, and it is less sensitive to precipitation data. To compensate for such data scarcity, SRM estimates discharges using remotely sensed snow cover data as basic input. For zone-wise approach, the discharge generated from each zone is summed up by SRM to simulate the flow from the entire catchment.

3.1.2. Satellite remote sensing data. Two important satellite-based data were used in SRM, i.e., topographic characteristics based on DEM and snow cover maps of the studied region. The data processing was simplified according to SRM format requirement by integrating the Python Programming codes and ArcGIS-Pro software developed by "Environmental System Research Institute" (ESRI).

"Digital Elevation Model (DEM)" provides data for acquiring the topographical characteristics of the study area and for the extraction and delineation of watersheds and are significant for hydrological simulations [37]. In addition, it can also be utilized to create a hypsometric (area-elevation) curve. "Shuttle Radar Topography Mission (SRTM) provides DEM with a spatial resolution of ~30 m and a near global coverage [38] and can be accessed through the "United States Geological Survey (USGS)" Earth Explorer web data portal in addition to other portals. For this study, the void filled SRTM DEM was downloaded from the online data portal https://portal.opentopography.org/datasets. This DEM was treated to delineate the watershed, streamlines, specific elevation zones (Fig 1) and to develop the hypsometric curve (S1 Fig) to visualize the catchment's mean elevation and area distribution under various elevation zones. Basin-wide and zone-wise topographical characteristics of the study area estimated from the DEM, are presented in Fig 1 and Table 1.

"Moderate Resolution Imaging Spectroradiometer (MODIS)" is an advanced satellite sensor onboard two NASA satellites namely "Terra" (launched in 1999) and "Aqua" (launched in 2002) in addition to several other sensors. Due to their synchronized orbits, Terra and Aqua together offer complementary data sets every 1–2 days, providing global coverage thereby making MODIS data essential to get insights into Earth's climate, hydrology and land dynamics [39,40]. In the current study, an "Improved MODIS TERRA/AQUA composite snow and glacier (RGI 6.0) data" for the study period 2005–2015 was utilized for the snow cover estimation. This improved and cloud free MODIS data was developed [41,42] by taking MOD10A2.006 (Terra product) and MYD10A2.006 (Aqua product) 8-day Composite collection 6 (C6) as input. This data is developed for High Mountain Asia (HMA) (latitude 24.32 − 49.19 N and Longitude 58.22 − 122.48 E) and it contains the MODIS snow cover merged with Randolph Glacier Inventory (RGI 6.0), the accuracy of which is reported by Pfeffer et al. [43]. The cloud-free MODIS data "MOYDGL06*" is therefore an improved snow cover and glacier combined product that is available from 2002 to 2021 [44]. The data is available with 8-day temporal and 500 m spatial resolution and was freely accessed through online data portal "https://doi.pangaea.de/10.1594/PANGAEA.901821" [41]. Although MODIS data has a coarser spatial resolution for complex terrain, but it is validated by the previous studies [45–49] with high-resolution sensors and is found as a reliable option for hydrological simulations for snow and glacier dominated mountainous basins [5,26]. The delineated Swat watershed and various elevation zones were used as a mask to extract the basin-wide and zone-wise snow cover over the data period 2005–2015 using python codes and ArcGIS Pro. Daily values of snow cover were then calculated by linear interpolation between 8-days MODIS images. Pixel values in this data are represented by Digital Numbers and are explained in Table 4.

The pixel value of 25 representing "no snow" in the extracted MODIS images were ignored while the pixel counts representing snow and glacial cover, i.e.,198, 199, 200, 238, 239, 242, 248, 249, 250 and 252 were used to estimate the snow and glacier cover. The snow and glacier cover area were determined from these pixel values by using equations

Table 4. Pixel values (codes) and their description for the MOYDGL06* improved snow and glacier product [50,51].

Pixel value	Feature in combined product	Pixel value	Feature in combined product
25	No snow	240	Exposed debris
198	Snow in Terra	242	Debris cover under Terra and Aqua snow
199	Snow in Aqua	248	Clean ice under Terra snow
200	Snow in both Terra and Aqua	249	Clean ice under Aqua snow
238	Debris under Terra snow	250	Exposed ice
239	Debris under Aqua snow	252	Clean ice under Terra and Aqua snow

https://doi.org/10.1371/journal.pclm.0000739.t004

mentioned in [42]. When calculating total snow and glacier cover on a given date, a weight of 0.5 was used for snow pixel if it was present in either the Terra or Aqua product described by values 198, 199, 238, 239, 248, and 249 and a weight of 1 for the pixels with snow in both the Terra and Aqua products with values 200, 242, 250 and 252.

3.2. Methodology

The detailed methodological steps adopted for this study are presented in Fig 2.

3.2.1. Snowmelt runoff model. The windows-based snowmelt-runoff model (Win-SRM) was used to simulate the daily discharges of the Swat River. SRM, a degree-day (temperature index) hydrological model, developed by Jaroslav Martinec, is widely used for the mountainous basins where snowmelt is the significant source of water [14]. It can be applied to any size of mountain basins ranging from 0.76 to 917,444 km^2 and any elevation range by accommodating up to 16 elevation zones of the basin [52]. Initially, it was applied for the small European (43 km^2) Dischma basin in eastern Switzerland [14], however, with the increasing availability of remote sensing data for snow cover, SRM is now being applied to larger basins [53]. This model can evaluate the effect of climate change on seasonal snow cover and runoff [53] and has successfully undergone the runoff simulation tests by the World Meteorological Organization [2].

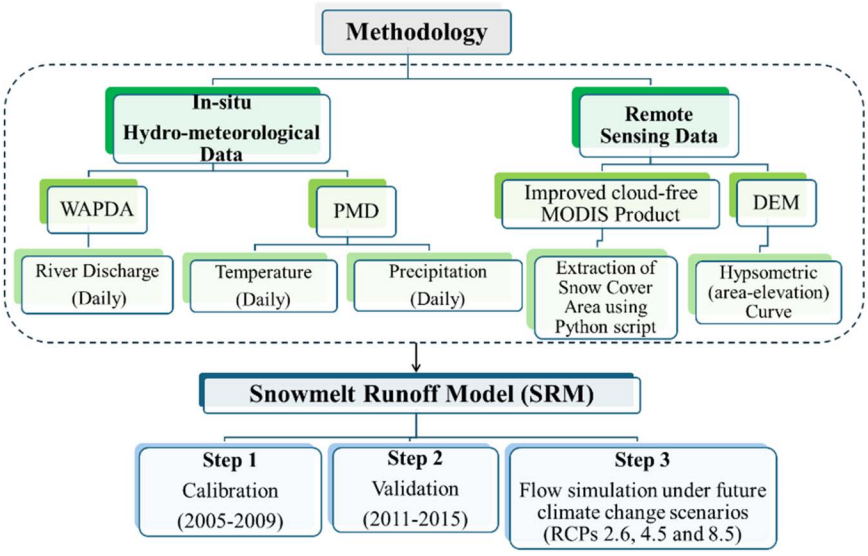

Fig 2. Flowchart outlining the systematic approach employed in research methodology.

https://doi.org/10.1371/journal.pclm.0000739.g002

Input variables include daily precipitation, air temperature and snow cover area. Additionally, the basin area, zone area (in zone-wise application) and the hypsometric (area elevation) curve are also required. The input variables and eight parameters to be calibrated for a successful simulation of daily discharge using SRM are given in Table 5.

The governing equation used for superimposing the daily water produced from the snowmelt and rainfall on the calculated recession flow, for transforming it into daily discharge from the catchment, is given as equation 1 [53].

$$Q_{n+1} = [c_{Sn}.\ a_n\,(T_n + \Delta T_n)\,S_n + c_{Rn}P_n]\,\frac{A\ .\ 10000}{86400}\,(1 - k_{n+1}) + Q_n k_{n+1} \tag{1}$$

where Q_{n+1} = Runoff at time step n + 1 (e.g., daily runoff in m³/s); C = the runoff coefficient expressing the losses as a ratio (runoff/precipitation, with C_{Sn} referring to snowmelt and C_{Rn} to rain; a = the degree day factor, DDF (cm.°C^{-1}.d^{-1}) indicating the snowmelt depth resulting from 1 degree-day; T_n = the number of degree-days (°C.d), ΔT_n = the adjustment by temperature lapse rate when extrapolating the temperature from the station to the average hypsometric elevation of the basin or zone (°C.d); S = the ratio of the snow covered area (SCA) to the total area; P = the precipitation contributing to runoff (cm); n = the sequence of days during the discharge computation period; A = the area of the basin or zone (km^2), K_{n+1} = the recession coefficient (X_c and Y_c) indicating the decline of discharge in a period without snowmelt or rainfall. A pre-selected threshold temperature, T_{crit}, determines whether this precipitation is rainfall and immediately converts it into runoff when $T > T_{crit}$, however, it is stored as snow if the $T < T_{crit,}$ until the melting conditions occur.

Two distinct accuracy criteria are employed to assess the efficiency of SRM to simulate the daily flow: i) "difference of volume (D_v)" and ii) "Nash-Sutcliffe Efficiency (NSE) Coefficient". The formulas for their computation are given below in equations 2 and 3:

$$D_v\ (\%) = \frac{V_R - V'_R}{V_R} \times 100 \tag{2}$$

Where, "V_R" is seasonally or yearly measured runoff volume, and "V'_R" is seasonally or yearly simulated runoff volume.

$$NSE = 1 - \frac{\sum_{i=1}^{n}(Q_i - Q_i)^2}{\sum_{i=1}^{n}(Q_i - \overline{Q}i)^2} \tag{3}$$

Where, "Q_i" is the average measured discharge of the given year or snowmelt season, "n" is the number of daily discharge values [54,55].

In this study, the snowmelt-runoff model was applied using two approaches: a basin-wide approach, treating the entire catchment as a single unit, and a zone-wise approach, dividing the basin into elevational zones to account for altitude-dependent variations in temperature, precipitation, and snow cover. To simulate the basin-wide and zone-wise daily discharge,

Table 5. Variables and Parameters used in SRM and their units.

Variables (Daily)	**Temperature, T (minimum and maximum or average); (°C)**	**Daily snow-covered area, Daily SCA; (Fraction value)**
	Precipitation, P (Centimeters-cm)	**Discharge, Q; (Cubic meter per second $\frac{m^3}{s}$)**
Parameters	Temperature lapse rate, γ; (°C/100m)	Rainfall contributing area (RCA)
	Degree day factor, *a;* (cm.°C^{-1}.d^{-1})	Recession coefficient (k)
	Critical temperature, T_{crit}; (°C)	Rainfall runoff coefficient (c_r)
	Time lag (hours)	Snowmelt runoff coefficient (c_s)

https://doi.org/10.1371/journal.pclm.0000739.t005

the SRM was calibrated over the data years 2005–2009 by adjusting the parameters (Table 5) and validated over 2011–2015. Considering the changes in the physical environment with altitude [2,3,56], the zone-wise application was used by reclassifying the Swat River Basin (SRB) into four elevation zones, i.e., A, B, C and D (Fig 1 and Table 1), where Zone A is the lowest elevation zone (681–1500 m ASL) and zone D is the highest elevation zone (3501–5898 m ASL). The best parameter values were determined by taking assistance from the published literature for the region where the catchment area is situated or by theoretical judgment [26]. Due to uncertainties in the variable values particularly discharge, the year 2010 was excluded from the analysis. The best suited parameters were obtained after many runs of the SRM to simulate the flow of the Swat River.

3.2.2. Integration of climate change scenarios in the calibrated SRM. Calibrated and validated SRM was integrated with climate change scenarios to predict future flow under varying climatic conditions. Representative Concentration Pathways (RCP) climate change scenarios (Table 6) statistically downscaled for the Indus River Basin (IRB) for the mid- and late-21st century [6], were used to assess the annual and seasonal summer flows. Many researchers have leveraged these downscaled RCP scenarios for estimating the projected changes in river flows in different basins [2,4,26,57–59]. Su et al. [6] compared the simulation results of CMIP5 (Coupled Model Inter-comparison Project phase 5) multi-model ensemble in the Indus River Basin (IRB) with the CRU (Climatic Research Unit) and APHRODITE (Asian Precipitation-Highly-Resolved Observational Data Integration Towards Evaluation) datasets. The equidistant Cumulative Distribution Functions matching method (EDCDFm) was applied to correct the systematic bias between simulations and observations, and high-resolution simulations were statistically downscaled. This process effectively tailored global climate models to the IRB's complex topography and seasonal variations, enabling region-specific impact assessments. Projections for precipitation and temperature within the IRB were subsequently developed, encompassing the mid-21st century (2046–2065) and the late-21st century (2081–2100). Table 6 shows variations in average annual and seasonal summer precipitation and temperature under RCPs scenarios.

4. Results and discussion

4.1. Spatio-temporal variations in the hydro-meteorological variables

Hydro-climatological data of the Swat River Basin is presented in Figs 3-5, which shows mean monthly discharge, total monthly precipitation, mean monthly temperature and mean monthly snow cover area (SCA) over a period of 2005–2015.

4.1.1. Variation in basin-wide temperature, precipitation, discharge and snow cover area. The overall basin-wide hydro-meteorological characteristics of SRB over 2005–2015 are demonstrated in Fig 3 revealing the variations in monthly mean temperature, total precipitation, discharge and snow cover area. The mean annual temperature of the basin was estimated to be ~ 17 °C, with overall the highest mean monthly temperature observed in the month of July (~27 °C) and lowest mean monthly temperature in the month of January (~6.5 °C) over the data period of 2005–2015 (Fig 3). Over the course of the year, two distinct phases of change are observed in the mean monthly temperature. The first is a sharp rise beginning in February, with temperatures increasing at a rate of ~4.8 °C per month until May. After this, the rate of

Table 6. Annual and seasonal summer variation in mean temperature and precipitation for mid-21st (2046–2065) and late-21st century (2081–2100) in the IRB [6].

Time Period	RCP Scenarios	Mean Annual		Mean Seasonal (summer)	
		Temperature (°C)	Precipitation (%)	Temperature (°C)	Precipitation (%)
Mid-21st century (2046–2065)	2.6	1.21	3.2	1.24	1.6
	4.5	1.93	0.1	1.90	3.2
	8.5	2.71	6.2	2.58	9.5
Late-21st century (2081–2100)	2.6	1.10	5.6	1.14	3.8
	4.5	2.49	4.0	2.38	7.3
	8.5	5.19	7.8	4.82	16.5

https://doi.org/10.1371/journal.pclm.0000739.t006

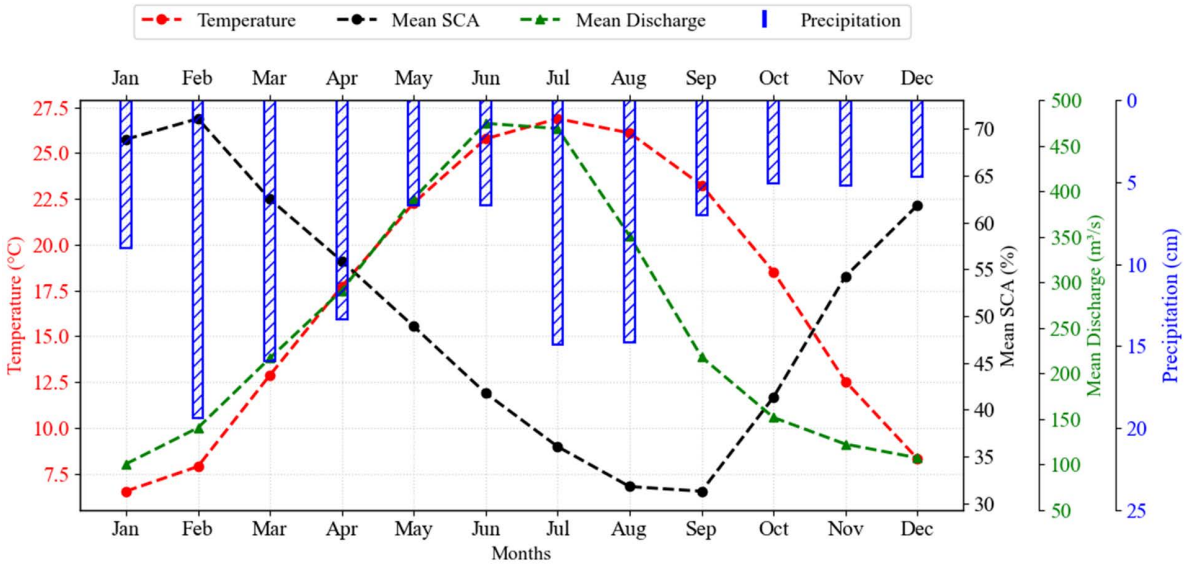

Fig 3. Basin-wide hydro-climatological data of the Swat River Basin (SRB) showing monthly mean discharge and total precipitation, monthly mean temperature variation and monthly mean snow cover area (SCA) over the data period 2005–2015.

https://doi.org/10.1371/journal.pclm.0000739.g003

increase slows, and temperatures peak in July. From August to December, temperatures decline rapidly at a rate of ~5 °C per month, followed by a slower decrease that continues until the lowest temperatures are reached in January. This temperature variation plays a key role in the runoff generation from the snow and glacier melting in the study area. Lowest specific mean monthly temperature value was recorded as ~4.13 °C in January 2012, and the highest temperature as ~28.12 °C in July 2014.

The lowest mean monthly temperature and ultimately the lowest discharge is found in January. This is because the winter discharge from November-January is generated through low melting induced by low temperatures with no significant contribution by the rainfall-runoff. On the other hand, the peak monthly mean temperature and discharge was found in June-July. The reason for this maximum discharge is higher temperature causing accelerated melting overlapped by the summer monsoon rainfall-runoff.

The average of total annual precipitation was ~ 122 cm (1220 mm) as estimated from the data. The maximum of total precipitation occurs during the February–April months (~49 cm) followed by June-September (~43 cm). Maximum value of monthly total precipitation of ~43 cm was recorded in July of 2010. This was the exceptional case and caused catastrophic floods in 2010 in the study area. Otherwise, the maximum monthly precipitation values were found in February 2011 (~30 cm) and March 2014 (~29 cm). For the total monthly precipitation (Fig 3), it is observed that there are two precipitation seasons influencing the study area: the westerly weather pattern bringing precipitation from February to April and summer monsoon from June to September [3,26].

The mean annual discharge over the study period was estimated to be ~ 253 m^3/s. It is found that the highest discharge occurs in the months from May-August with highest mean flow in the month of June (~474 m^3/s). The rising temperatures in summers cause rapid melting of snow which ends up magnifying the discharge in the Swat River. Conversely, months with minimum flow, span from November to February with lowest mean discharge in January (~100 m^3/s). Freezing minimum temperatures, excessive snowfall due to westerlies and reduced snowmelt decelerate the water flow from the mountains, thereby resulting in less discharge during winters. The river flow begins to increase as the temperature starts rising in late winter and peaking in summer (June-July), demonstrating the primary discharge of SRB driven by snowmelt

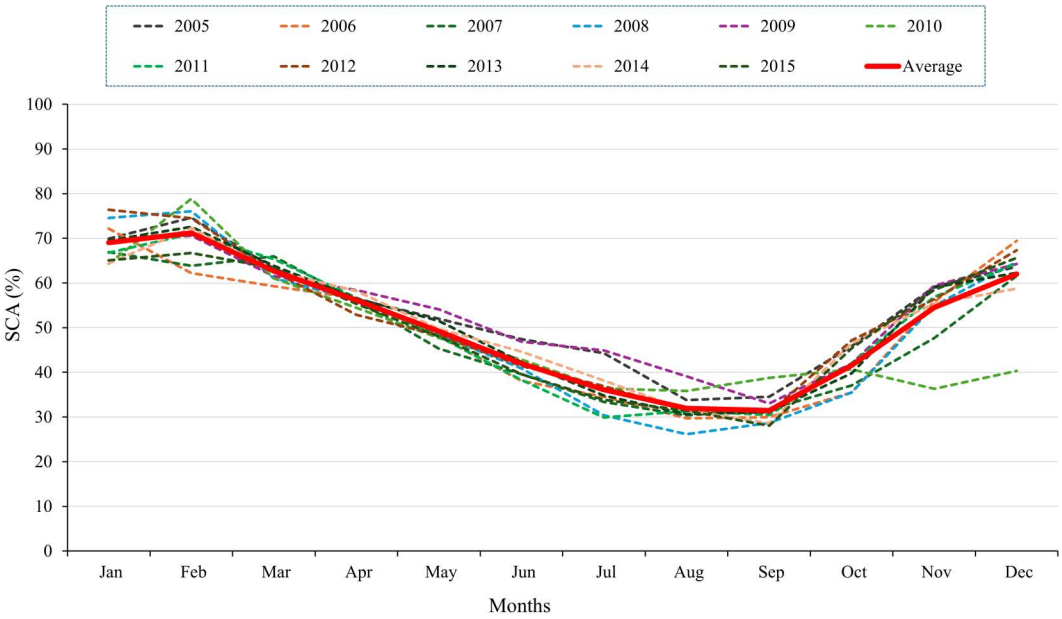

Fig 4. Mean monthly basin-wide snow cover variation over the period of 2005–2015 in the study area.

https://doi.org/10.1371/journal.pclm.0000739.g004

from spring to early summer [60], and by sustaining the summer discharge due to remaining snow-glacier melt and monsoon precipitation. Such hydro-climatological profile of SRB is aligned with the defining characteristics of mountainous and snow dominated river basins.

Temporal variations in basin-wide mean monthly SCA of Swat River Basin are shown in Fig 3 (mean monthly of entire data period) and Fig 4 (mean of each data year). Mountainous basins like Swat River Basin are characterized by gradual decline in spatial extent of seasonal snow cover during snowmelt season. Overall, it is found that in the SRB, snow accumulates from October to February, followed by melting from March to September, showing a declining trend. Analysis indicates a mean annual SCA of ~50%, peaking at ~72% in February and reaching a low of ~31% in September. February's maximum SCA is due to westerly winds causing heavy snowfall (Fig 3) at higher elevations and persistent cold that slows down the melting process. Conversely, summer's high temperatures drive extensive melt, leading to September's minimum SCA. Spatially, northern slopes in the basin have a consistent snow cover year-round (Fig 5) due to higher elevation zones in the north as apparent from the DEM (Fig 1) and thus lower mean temperatures, while southern slopes have lower elevation zones experiencing higher mean temperatures causing snow to melt faster hence lower mean annual snow coverage. Maximum mean annual SCA of ~54% was observed during 2005 whereas 2010 was the year with least mean annual SCA of ~48% (Fig 4).

4.1.2. Variation in zonal SCA and mean temperature. In zone-wise application of SRM, daily zonal SCA and zonal mean temperature are used as basic input. The average of the basin's daily total precipitation may be used in each zone if the zonal precipitation data is not available knowing that the SRM is less sensitive to precipitation input. Zonal SCA was estimated from improved MODIS data, while the zonal mean temperature at the hypsometric mean elevation of each zone was estimated by using the basin's temperature lapse rate value for all four elevation zones (A, B, C, and D) of the Swat River Basin over the study period. The radar graph (Fig 6) illustrates the monthly mean SCA and mean temperature variation for all elevation-based zones.

A clear seasonal snow cover pattern across all the zones is evident in Fig 6a with distinct variations in magnitude and duration among them. Zone D maintains the highest mean monthly snow cover (~97.5–100%) from November to May. Zone D is the highest elevation zone where the colder temperatures, governed by the environmental lapse rate, are

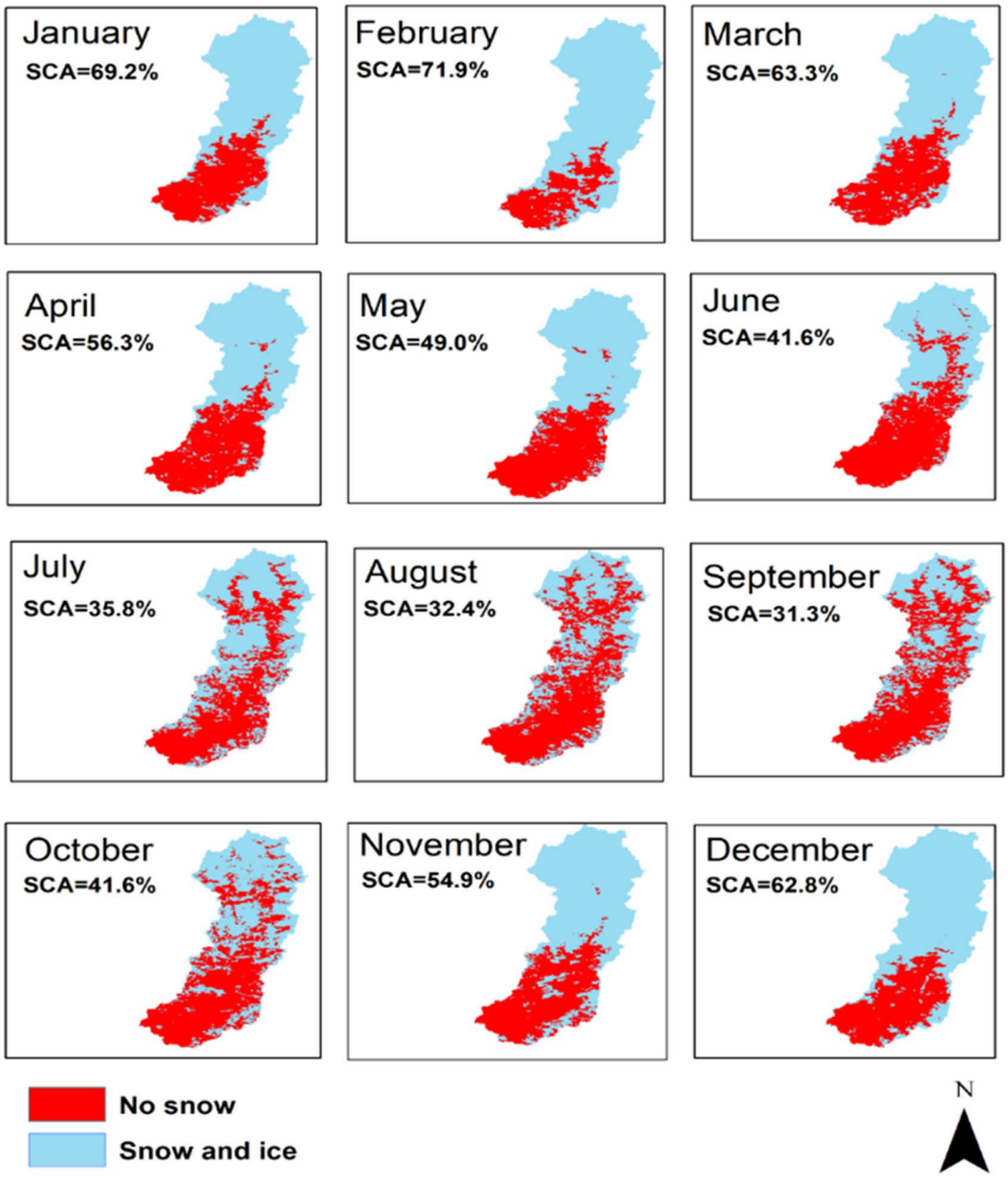

Fig 5. Spatial variation in the basin-wide mean monthly SCA of the Swat River Basin over data period 2005–2015.

https://doi.org/10.1371/journal.pclm.0000739.g005

responsible for the precipitation in the form of snow and its prolonged retention over months [2,61]. On the other hand, Zone A demonstrates minimal mean snow cover, with a peak slightly exceeding ~12% in January signifying its warmer, lower-elevation status. Zone B and Zone C demonstrate peak SCA in February, i.e., ~68% and ~100%, respectively. Mean (minimum-maximum) annual SCA for zone A, B, C and D were found to be ~5% (~1–12%), ~31% (~12–67%), ~65% (~29–100%), and ~88% (~57–100%), respectively, over data period 2005–2015.

Fig 6a clearly depicts the snow accumulation phases, evident from October through December, and peaking in January and February. Conversely, the significant decline from March onwards indicates the melt season, accelerating into late

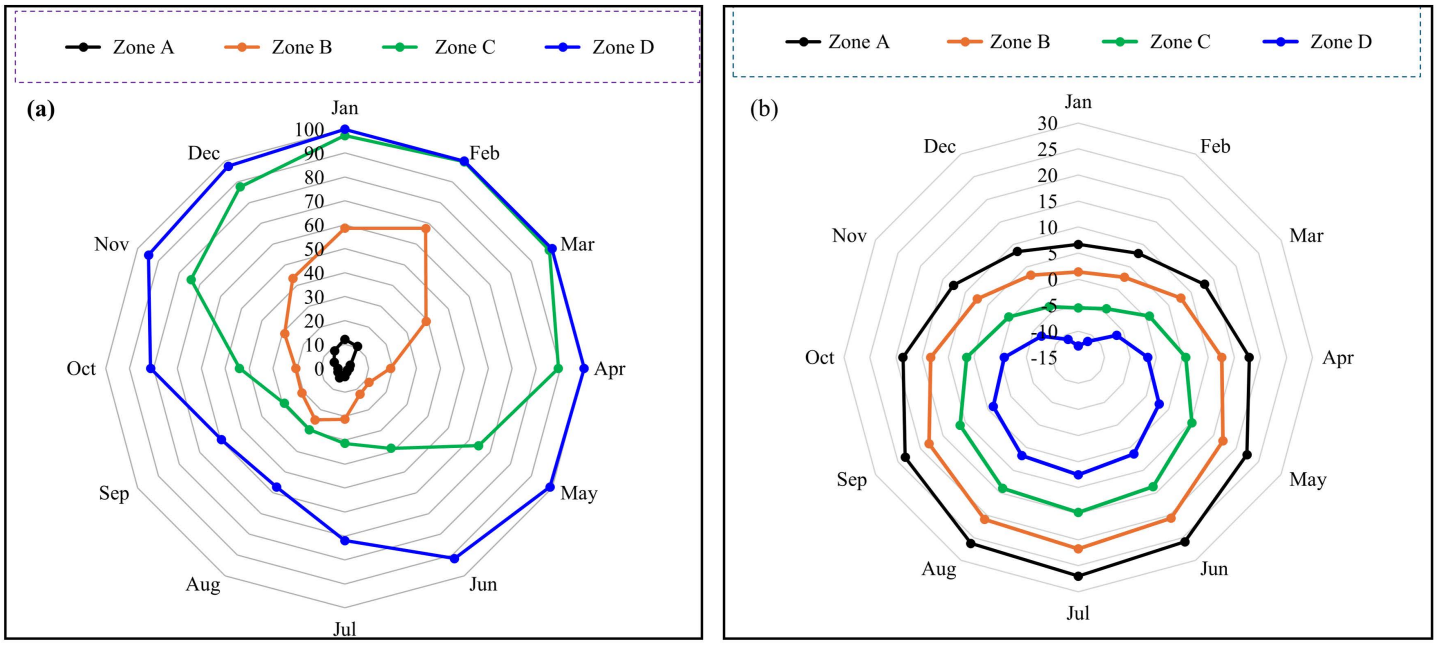

Fig 6. Mean monthly zonal (a) SCA, and (b) temperature variations in the Swat River Basin during 2005–2015.

https://doi.org/10.1371/journal.pclm.0000739.g006

spring and early summer (May-July). High flow values from June-September also indicate an overlapped monsoon season. This signifies the seasonal transition from snowmelt-dominated runoff to rainfall-driven or baseflow contributions [62]. Such distinct zone-wise stratification indicates the significant influence of elevation or climatic differences influencing snow accumulation and melting within the basin [53].

The zone-wise mean monthly temperature variation is presented in Fig 6b. Mean (minimum-maximum) annual temperature for zone A, B, C and D were found to be ~ 17.5 °C (~6.6–27 °C), ~ 12.2 °C (~1.4–22 °C), ~ 5.3 °C (~-5.6–14.8 °C), and ~-1.96 °C (~-12.8–7.5 °C), respectively, over data period 2005–2015. Zone A (lowest altitude) is found to have the highest mean annual temperature while Zone D (highest altitude) has the lowest mean annual temperature. However, the variation in temperature during the year shows maximum monthly temperature in July and minimum monthly temperature in January for all the zones.

4.2. Basin-wide and zone-wise simulation of historical daily discharge (2005–2015)

Daily river flow from Swat River Basin was simulated by applying basin-wide and zone-wise SRM over the data period of 2005–2015 for the melt season (April to September). Both the basin-wide and zone-wise SRM approaches were carried out using the daily hydro-meteorological variables including the SCA. Several parameter values were adopted from previous studies [2,3,5,63] on mountainous basins of the UIB, while others were adjusted during calibration to reflect seasonal variations in temperature, precipitation, and snow conditions in specific months. These adjustments were constrained within logical ranges consistent with values reported in the literature for the hydrological response of mountain catchments. The best calibrated parameter values used for simulating river discharge from Swat River Basin are presented in Table 7.

A range of DDF (0.3–0.65 cm.°C^{-1}.d^{-1}) was obtained for SRB due to certain factors like seasonal variation (more ablation during hotter months) and difference in characteristics of snow and ice (snow density, albedo effect, thermal properties). The lag time refers to the time taken between the occurrence of a rainfall or snowmelt event and the resulting runoff

Table 7. Parametric values of SRM for simulation of basin-wide and zone-wise river discharge from the Swat River Basin.

Parameters	Basin-wide	Zone-wise			
		Zone A	Zone B	Zone C	Zone D
Temperature lapse rate, ΔT; (°C/100m)	0.66	0.66	0.66	0.66	0.66
Critical Temperature, T_{crit}; (°C)	0	0	0	0	0
Degree day factor, *a*; (cm.°C^{-1}.d^{-1})	0.3–0.45	0.35–0.65	0.35–0.65	0.35–0.65	0.35–0.65
Lag time, (h)	10–15	12	12	12	12
Snowmelt runoff coefficient, C_s	0.13–0.4	0.23–0.6	0.23–0.6	0.23–0.6	0.23–0.6
Rainfall runoff coefficient, C_r	0.12–0.4	0.15–0.5	0.15–0.5	0.15–0.5	0.15–0.5
Rainfall Contributing Area, RCA	0 = No Rain, 1 = Rain	0 = No Rain, 1 = Rain	0 = No Rain, 1 = Rain	0 = No Rain, 1 = Rain	0 = No Rain, 1 = Rain
X_c	0.09–1.08	0.996–1.08	0.997–1.08	0.997–1.08	0.997–1.08
Y_c	0.005–0.08	0.017–0.04	0.017–0.03	0.017–0.03	0.017–0.03

https://doi.org/10.1371/journal.pclm.0000739.t007

to reach the farthest point in the watershed. Therefore, time lag is usually small for a smaller basin and more for larger ones [53]. A range of time lag, (10–15 hours) was taken for the Swat River Basin to ensure that the model accurately captures various factors influencing water movement in this mountainous basin. The runoff coefficients, C_s and C_r, were adjusted according to the months with a dominant pattern of contribution from the snowmelt or rainfall. Similarly, RCA (Rainfall Contributing Area) was taken 1 in the months when rainfall events are frequent in the basin, i.e., February-April and July-August while it was taken 0 in the months when snow is dominant. Lastly, X_c and Y_c recession coefficient values were used to adjust the time and magnitude of peaks for fine tuning of the simulated curve.

Table 8 presents SRM's efficiency over calibration and validation periods using basin-wide and zone-wise application for the simulation of river discharge. This approach ensured that the SRM parameters efficiently captured inter-annual variability in runoff response. Overall, the SRM showed strong predictive performance, aligning with its recognized effectiveness in simulating the discharge for the snow and glacier dominated mountainous catchments [3,26]. For the basin-wide approach, the highest NSE of 0.95 was achieved particularly in 2005 and 2014 indicating significantly a high alignment between simulated and observed runoff during these years. While the lowest NSE (0.82) for the basin-wide approach occurred in 2006, still expressing a highly acceptable model performance [53]. In case of volume difference, the basin-wide approach showed its best performance in 2012 with $D_v = 0.03\%$, however the major deviation as an underestimation was indicated in 2011 with $D_v = -3.64\%$.

The calibration and validation phase demonstrated satisfactory outcomes as can be seen from the basin-wide and zone-wise values of D_v and NSE in Table 8. Likewise, for the zone-wise approach, the highest NSE (0.93) was observed in 2005 (during calibration), with the lowest (0.80) was recorded in 2011 and 2013, i.e., during the validation. Volume differences for the zone-wise method were negligeable in 2007 (~0.03%), however the model showed large underestimation of -4.56% in 2013. The model efficiently simulated the year 2007 discharge with basin-wide (zone-wise) approach presenting a $D_v = 0.61\%$ (0.03%) and NSE = 0.93 (0.91), hence it was chosen as base-year for simulation of future discharge under RCPs. The minor year-to-year fluctuations in model performance likely result from varying quality of input data or the occurrence of extreme weather events and shifts in how snowmelt contributed to runoff each year may not be fully captured by SRM.

Figs 7 and 8 illustrate the SRM's model performance across the calibration (2005–2009) and validation period (2011–2015) by comparing the simulated and observed discharge for the basin-wide and zone-wise application, respectively. The model's ability to capture the temporal dynamics of discharge is evident from the close agreement between the simulated (red line) and measured (blue line) hydrographs.

For the basin-wide application (Fig 7), the average value of NSE was 0.90 and 0.87 with volume differences (D_v) of 0.51% and -1.31% during calibration and validation, respectively. Similarly, for the zone-wise application (Fig 8), the average NSE was 0.91 and 0.84 with D_v values of -0.83% and -2.27% during calibration and validation, respectively. Hence, for the basin-wide (zone-wise) application, the average NSE and D_v over the entire data period (2005–2015) were 0.88(0.87) and -0.40% (-1.5%), respectively. These metrics indicate a reliable fit between observed and simulated discharge during the calibration for both applications and demonstrate that the model's predictive competence remained substantial, though slightly reduced, when applied to data periods not used during its initial calibration. The D_v values suggest a slight overestimation of total water volume during basin-wide calibration and a slight underestimation in both validation periods, with a more noticeable underestimation in the zone-wise validation. Overall, the SRM model demonstrates a convincing ability to simulate discharge across both basin-wide and zone-wise scales.

Table 8. SRM's efficiency over calibration (2005–2009) and validation (2011–2015) period using basin-wide and zone-wise application for simulation of river discharge in the study area.

	Year	Basin-wide		Zone-wise	
		Difference of Volume (D_v) (%)	Nash-Sutcliffe Coefficient (NSE)	Difference of Volume (D_v) (%)	Nash-Sutcliffe Coefficient (NSE)
Calibration	2005	1.16	0.95	-0.76	0.93
	2006	-2.95	0.82	-1.84	0.88
	2007	0.61	0.93	0.03	0.91
	2008	0.84	0.92	-2.40	0.91
	2009	2.91	0.87	0.83	0.90
Validation	2011	-3.64	0.83	-3.85	0.80
	2012	0.03	0.85	0.24	0.85
	2013	-1.89	0.87	-4.56	0.80
	2014	1.16	0.95	-4.07	0.91
	2015	-2.19	0.84	0.91	0.82

https://doi.org/10.1371/journal.pclm.0000739.t008

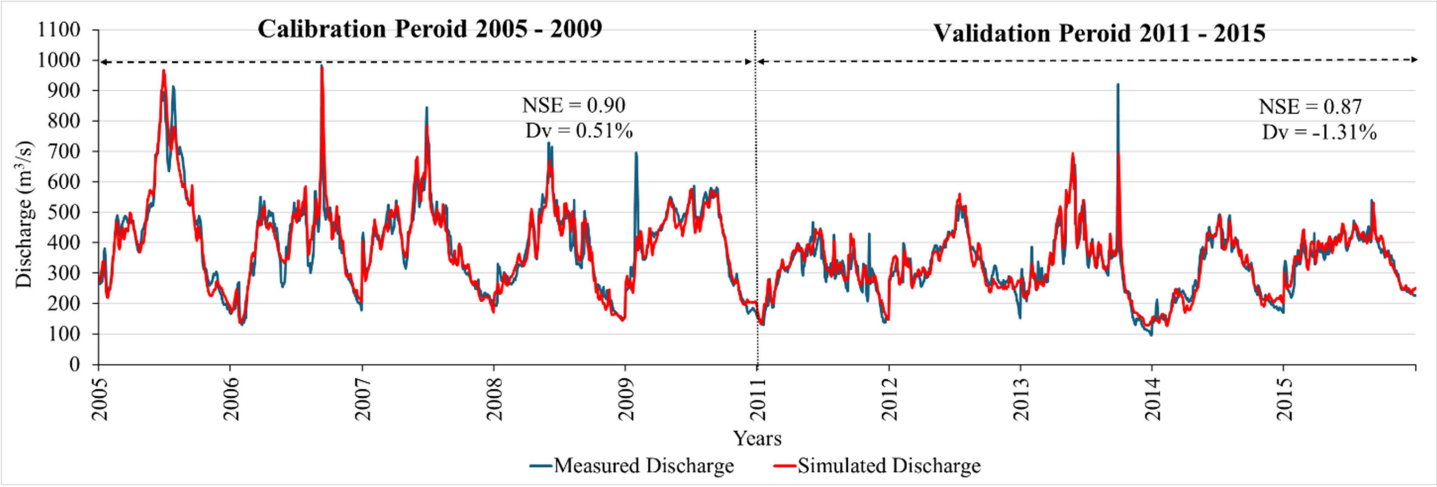

Fig 7. Basin-wide evaluation of SRM efficiency in simulating melting season (April to September) river discharge during the calibration (2005–2009) and validation (2011–2015) period for the Swat River Basin.

https://doi.org/10.1371/journal.pclm.0000739.g007

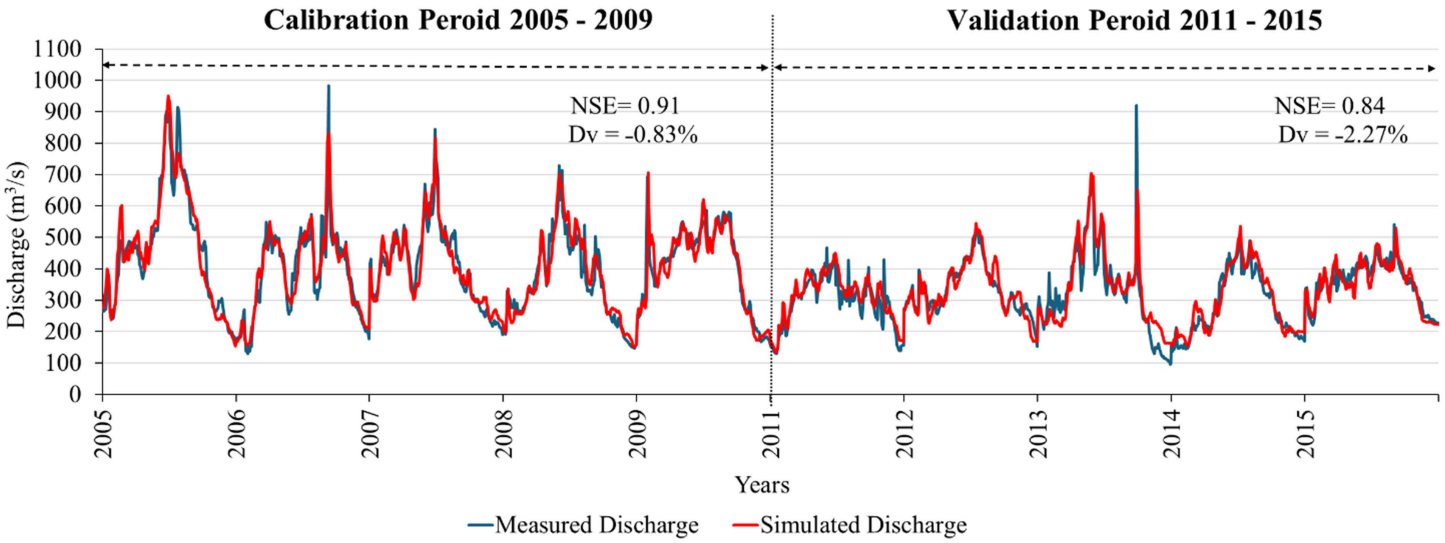

Fig 8. Zone-wise evaluation of SRM efficiency in simulating melting season (April to September) river discharge during the calibration (2005–2009) and validation (2011–2015) period for the Swat River Basin.

https://doi.org/10.1371/journal.pclm.0000739.g008

A correlation (Coefficient of Determination, R^2) between the observed and simulated runoff of the Swat River Basin over the entire data period of 2005–2015 (excluding 2010) is shown in Fig 9. This correlation demonstrates the strong ability of the SRM to simulate discharge in the Swat Basin, at the basin-wide and zone-wise scale.

The simulated discharge shows a close alignment between $R^2 = 0.91$ for basin-wide (Fig 9a) and $R^2 = 0.91$ for zone-wise (Fig 9b). However, some scatters, particularly at higher discharge rates, suggest a degree of variability in the model's accuracy at peak flows. Fig 9c demonstrates the performance of the SRM model by illustrating the relationship between basin-wide and zone-wise simulated Swat River discharges. The red line represents the best-fit linear regression between these two approaches depicting the strong positive correlation ($R^2 = 0.93$). These results highlight the model's robustness in accurately simulating hydrological responses, upholding its suitability for both long-term discharge analysis and understanding spatial variations in discharge within the high-altitude mountainous basin such as SRB at basin-wide and zone-wise scales. However, lack of gauged weather data in such areas has contributed to the limitations in precisely capturing all discharge fluctuations which eventually affected the runoff simulation results.

Throughout the study, the basin-wide approach consistently delivered slightly better NSE values and showed more stable runoff volume differences compared to the zone-wise method, particularly during the validation period. This indicates that basin-wide SRM approach proves to be remarkably consistent and reliable in offering deeper insights into specific local processes as compared to the approach of dividing the basin into zones [3] for simulating the total discharge of the Swat River Basin. The improved performance of the basin-wide simulation over the zone-wise approach in this study can be attributed to several key factors. Basin-wide modeling offers a more integrated representation of hydrological processes, reducing complexity by requiring fewer parameters (only for one zone) and avoiding inconsistencies that may arise from subdividing the basin. It ensures continuity in snowmelt and runoff processes, minimizes the influence of localized input data anomalies or scarcity, error accumulation, data quality [3,57] and avoids irregular zonal boundaries that can distort flow dynamics. As a result, it delivers more stable and reliable discharge predictions, particularly evident during the validation period, as reflected in the higher NSE values and consistent runoff volumes. Other reasons could be that the hydrological processes can vary significantly with scale, that may cause a model to perform well at basin level but compromise in capturing the distinctions of unique hydrological characteristics of zones (smaller sub basins) [53]. Such

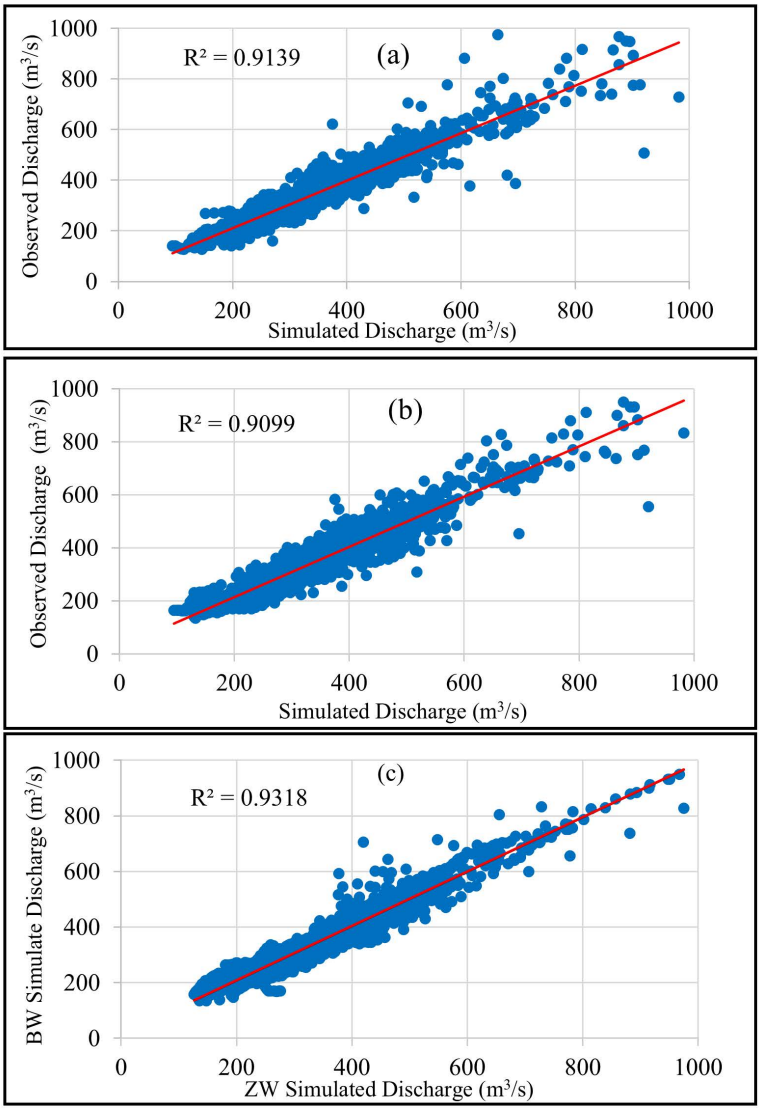

Fig 9. Correlation of measured and simulated discharge over a period of 2005–2015 for the (a) basin-wide application, (b) zone-wise application, and (c) between basin-wide and zone-wise simulated discharges.

https://doi.org/10.1371/journal.pclm.0000739.g009

as, the factors like precipitation, snowmelt, and land cover can exhibit more variability at the zone level. The model might struggle to capture the complexities and accurately represent this erraticism with the same set of variables used for the entire basin.

4.3. Impacts of climate change on the mean annual and summer flows under future RCPs climatic scenarios

The calibrated and validated SRM was applied to predict future annual and summer flow dynamics of the Swat River Basin under the climate change by applying the future RCP scenarios. Summer snowmelt season (April to September) being hydrologically significant was the focus of this investigation as the peak discharge responsible for flooding or filling the reservoirs happens during this period. The year 2007 was among the best, simulated with NSE > 0.93 and

this simulated flow was chosen as reference (base) year. For applying RCP scenarios on annual flow, the year of March 2007– April 2008 was simulated by adjusting the parameters resulting in NSE of ~0.97 and a D_v of ~2.5%. These RCPs assessed the impacts of increase in the mean temperature and average precipitation (annual and monsoon season) in the Swat River Basin for the mid- and late-21st century.

Figs 10a and 10b show that the mean annual river discharge is projected to increase by ~8%, ~12% and ~18%, while the mean melt season discharge is expected to increase by ~7%, ~11% and ~16% under mid-21st century RCPs 2.6, 4.5 and 8.5 scenarios, respectively. Figs 10c and 10d show that the mean annual flow is projected to increase by ~7%, ~16% and ~30%, while the summer (melt season) discharge is projected to increase by ~7%, ~15% and ~30% under late-21st century RCPs 2.6, 4.5 and 8.5, respectively. In addition, a 1 °C rise in mean temperature will cause an increase of ~7% in the mean annual flow and ~6% in the mean seasonal flow of the study area. These results indicate that the Swat River flow increases by approximately 6–7% for each 1 °C rise in temperature, which aligns well with previous studies reporting a 5–8% $°C^{-1}$ increase in discharge for snow- and glacier-fed basins in the Himalaya and European Alps [60,64–66]. This consistency highlights the strong temperature sensitivity of cryospheric catchments like the Swat Basin and reinforces concerns about increasing meltwater contributions under future warming scenarios. It is important to note that SRM does not explicitly account for dynamic glacier retreat, which may reduce melt contributions later in the century, nor does it incorporate ensemble climate forcing. In such cases, the projected increase in mean annual flows by late 21st century may be considered as upper-bound estimation under high emission scenario (RCP 8.5). Moreover, our projections should be viewed as indicative trends rather than precise forecasts for water-resources planning.

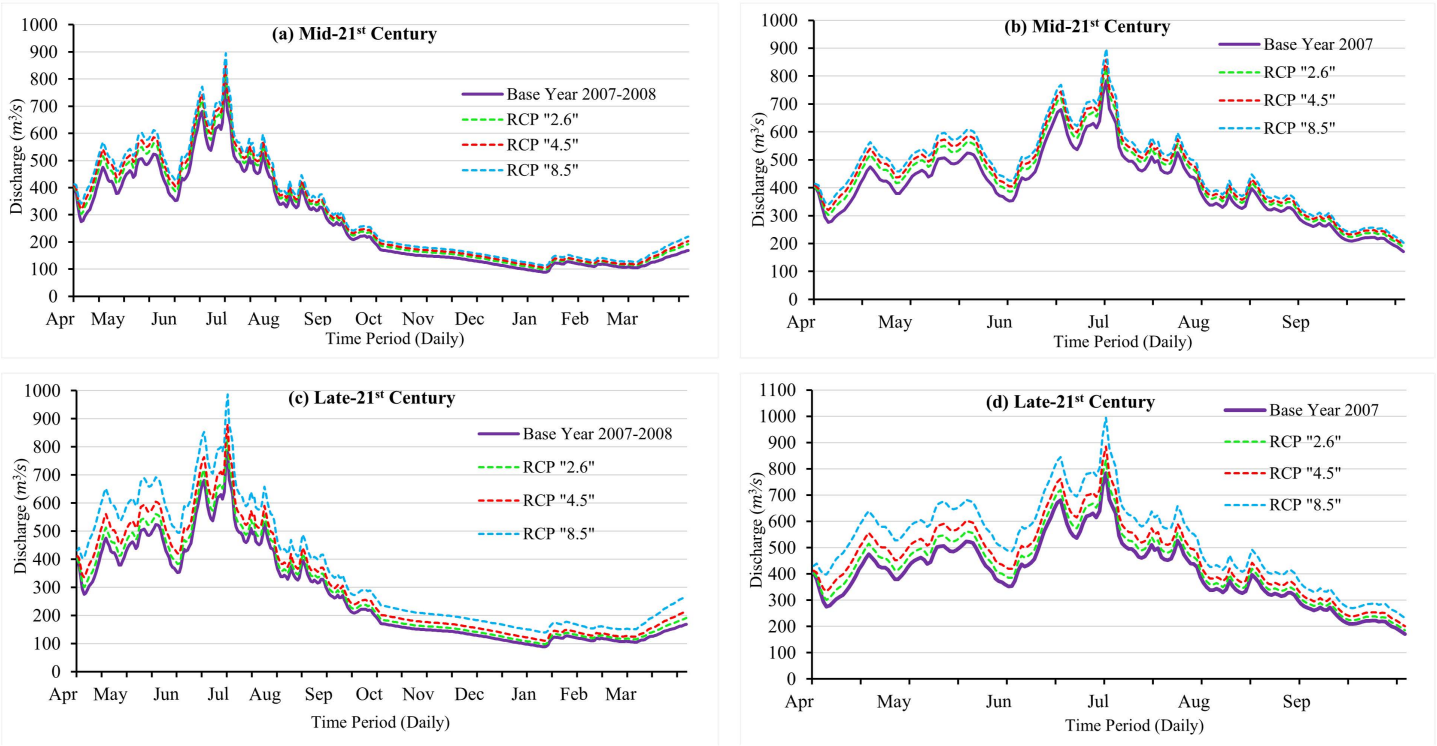

Fig 10. Simulation of annual (April-March) and summer (April-September) discharge under RCP climate change scenarios for the (a-b) mid-21st century (2046–2065) and (c-d) the late-21st century (2081–2100).

https://doi.org/10.1371/journal.pclm.0000739.g010

In the Swat River Basin, all RCP scenarios project an upward trend in discharge during early summer, coupled with reduced late-summer runoff, indicating a shift in snowmelt timing. The peaks in flow during June and July highlight climate-driven changes in snowmelt volume and timing, emphasizing the basin's high sensitivity to warming. These warming trends are expected to cause earlier snowmelt onset and increased discharge volumes, extending its effects into winter through elevated baseflows and accelerated melt dynamics [4,67]. However, if these scenarios come true, the glaciers situated in this basin may disappear and mean SCA may significantly reduce till the end of the century after producing accelerated flows. The magnitude of these changes varies with RCP scenarios, being most distinct under RCP 8.5, moderate under RCP 4.5, and lowest under RCP 2.6, reflecting the influence of climate change on snow and ice melting and the occurrence of extreme events like floods. Such changes can escalate the risk of flooding and erosion, challenges already evident in the region's hydrological records [6,68]. Furthermore, the anthropogenic activities (deforestation, urbanization and floodplain encroachment) further exacerbate these impacts by disrupting the natural flow and resilience of the basin, emphasizing its long-term vulnerability and the urgent need for adaptive water resource strategies to reduce basin's risk to hydro-meteorological hazards and disasters [35,69].

While SRB possesses a relatively smaller glaciated area, accurately modeling this contribution remains crucial for optimizing overall simulation performance. A recognized constraint of the SRM is its inherent inability to directly account for glacier-melt runoff, a process intricately shaped by factors such as ice thickness, surface albedo, and debris cover. However, employing a simplified degree-day methodology with consistent DDFs represents a well-established and widely adopted practice in high-mountain environments facing data scarcity such as UIB. This approach proves particularly practical where the detailed input required for physically-based energy balance modeling (e.g., glacier albedo, precise ice thickness, or debris distribution) is not feasible. To mitigate the typical uncertainties related to SRM, a DDF-based models, utilized for mountainous basins, the integrated cloud-free MODIS "MOYDGL06*" snow cover data was used, which helped in simulating the timing and magnitude of snowmelt more realistically, and assisted in addressing the issues of potential overestimation of runoff under warming scenarios. This study acknowledges that a more physically explicit representation of glacier-melt processes could be achieved through spatially and temporally variable DDFs or a full energy balance model. However, this level of detail exceeds the scope of this study which was centered on incorporating refined remotely sensed snow cover data designed for long-term hydrological projections under changing climatic conditions.

It is worth noting that structure of SRM does not explicitly capture the differences between debris-covered and clean ice surfaces or albedo variability and sub-monthly rain-on-snow events that can substantially alter runoff peaks [70,71]. This may miss the short-lived sharp peaks (e.g., flash floods or extreme runoff days) which are sensitive to glacier-melting process [71,72]. However, since glaciers in our study area are just 3.5% of basin, it will not change the overall basin water budget too much, hence, the overall results are still reliable. Furthermore, employing a spatially and temporally variable degree-day factor (DDF) or adopting an energy balance model could yield a more physically robust representation of glacier melt processes. Nevertheless, this lies beyond the scope of the present study, which instead emphasizes the integration of enhanced remotely sensed snow cover data into a parsimonious modeling framework designed for long-term hydrological simulations under climate change.

This study also acknowledges that although SRM is relatively less sensitive to precipitation due to higher reliance on remotely sensed snow cover data, the compromised precipitation data due to limited meteorological stations may cause bias into simulated runoff. Similar limitations have been reported by different studies [4,5,26]. Future studies can address this gap by incorporating gridded climate reanalysis and satellite precipitation datasets (e.g., CHIRPS, APHRODITE) to compete with limited ground observations and improve the spatial representations of meteorological inputs.

Lastly, it is worth noting that this study has successfully presented a hybrid methodology by coupling SRM with data driven techniques. Under the general concept of deep learning, computational accuracy was enhanced by using python-based scripts developed for the extraction of remotely sensed snow cover, while integrating it with ArcGIS Pro

software. Such deep learning and hybrid models may offer significant opportunities for future work that could complement process-based approaches like SRM.

5. Conclusions

This study employed SRM coupled with improved cloud-free snow and glacier composite products to simulate snowmelt runoff from snow- and glacier-fed Swat River Basin. The research investigated the future rise in river discharge by assessing how the cryosphere dynamics specifically snow, and glacier melt are altered by the rising temperatures and shifts in precipitation patterns projected under various 21st-century RCP climate scenarios.

The study confirms that: 1) SRM yields robust simulations of daily river discharge in snow-fed basins when integrated with improved snow cover products, with both basin-wide and zone-wise approaches performing well, though the basin-wide setup offered greater stability and reduced parameter uncertainty. 2) Model projections under RCP scenarios suggest substantial increases in river flows, with mean annual discharge expected to rise by ~8–18% in the mid-21st century and ~7–34% by the late 21st century, while summer flows may increase by ~7–16% and ~7–30% over the same periods. Additionally, a 1 °C rise in temperature is likely to enhance both annual and seasonal flows by ~6–7%, underscoring the sensitivity of the basin's hydrology to future climate warming. These findings suggest a heightened flood risk and shifting hydrological patterns, with all RCP scenarios projecting earlier peak flows in early summer followed by reduced flows in late summer highlighting the basin's pronounced sensitivity to climate warming. The likelihood of flooding may increase as rising regional temperatures accelerate the melting of snow and glacier, suggesting that the policy makers should focus on sustainable measures for the highly vulnerable downstream area and timely actions to minimize the flood destruction. Assessing future flood risks can be effectively achieved by integrating snowmelt runoff modeling with high resolution remote sensing data and climate change projections, particularly in data-scarce regions. In flood-prone northern Pakistan, enhancing flow prediction accuracy and implementing comprehensive flood management strategies especially non-structural measures like community awareness and disaster preparedness are essential for effective mitigation.

Supporting information

S1 Checklist. Data used in the research and displayed in figures and tables of the manuscript.
(DOCX)

S1 Fig. Hypsometric curve estimated from SRTM-DEM of the Swat River Basin, distribution of zones, and area percentage per 500 m elevation bands.
(ZIP)

Acknowledgments

The authors extend gratitude to the Water and Power Development Authority (WAPDA) and Pakistan Meteorological Department (PMD) for sharing the hydrological and meteorological data. We thank the PANGAEA data publisher and USGS for free access to improved MODIS snow data and SRTM DEM, respectively.

Author contributions

Conceptualization: Adnan Ahmad Tahir, Muhammad Irshad, Faizan-ur-Rehman Qaisar, Sher Muhammad, Muhammad Abrar Faiz.

Data curation: Esha Naeem, Wu Kunpeng.

Formal analysis: Romana Jamshed, Esha Naeem.

Funding acquisition: Adnan Ahmad Tahir, Wu Kunpeng.

Investigation: Romana Jamshed, Esha Naeem.

Methodology: Esha Naeem, Adnan Ahmad Tahir, Sher Muhammad.

Project administration: Sher Muhammad, Wu Kunpeng, Muhammad Abrar Faiz.

Resources: Adnan Ahmad Tahir, Muhammad Irshad, Sher Muhammad, Muhammad Abrar Faiz.

Software: Romana Jamshed, Esha Naeem, Adnan Ahmad Tahir, Wu Kunpeng.

Supervision: Adnan Ahmad Tahir, Muhammad Irshad, Faizan-ur-Rehman Qaisar, Awais Arifeen.

Validation: Romana Jamshed, Adnan Ahmad Tahir, Sher Muhammad.

Visualization: Sher Muhammad.

Writing – original draft: Romana Jamshed, Esha Naeem.

Writing – review & editing: Romana Jamshed, Esha Naeem, Adnan Ahmad Tahir, Muhammad Irshad, Faizan-ur-Rehman Qaisar, Awais Arifeen, Sher Muhammad, Wu Kunpeng, Muhammad Abrar Faiz.

References

1. Mukhopadhyay B, Khan A, Gautam R. Rising and falling river flows: contrasting signals of climate change and glacier mass balance from the eastern and western Karakoram. Hydrolog Sci J. 2015;60(12):2062–85. https://doi.org/10.1080/02626667.2014.947291
2. Tahir AA, Chevallier P, Arnaud Y, Neppel L, Ahmad B. Modeling snowmelt-runoff under climate scenarios in the Hunza River basin, Karakoram Range, Northern Pakistan. J Hydrol. 2011;409(1–2):104–17. https://doi.org/10.1016/j.jhydrol.2011.08.035
3. Hayat H, Tahir AA, Wajid S, Abbassi AM, Zubair F, Hashmi Z ur R, et al. Simulation of the meltwater under different climate change scenarios in a poorly gauged snow and glacier-fed Chitral River catchment (Hindukush region). Geocarto Int. 2019;37(1):103–19. https://doi.org/10.1080/10106049.2019.1700557
4. Hayat H, Akbar TA, Tahir AA, Hassan QK, Dewan A, Irshad M. Simulating Current and Future River-Flows in the Karakoram and Himalayan Regions of Pakistan Using Snowmelt-Runoff Model and RCP Scenarios. Water. 2019;11(4):761. https://doi.org/10.3390/w11040761
5. Khan U, Jamshed R, Tahir AA, Qaisar F ur R, Wu K, Arifeen A, et al. Anticipating Future Hydrological Changes in the Northern River Basins of Pakistan: Insights from the Snowmelt Runoff Model and an Improved Snow Cover Data. Water. 2025;17(14):2104. https://doi.org/10.3390/w17142104
6. Su B, Huang J, Gemmer M, Jian D, Tao H, Jiang T, et al. Statistical downscaling of CMIP5 multi-model ensemble for projected changes of climate in the Indus River Basin. Atmosph Res. 2016;178–179:138–49. https://doi.org/10.1016/j.atmosres.2016.03.023
7. Iqbal M, Dahri Z, Querner E, Khan A, Hofstra N. Impact of Climate Change on Flood Frequency and Intensity in the Kabul River Basin. Geosciences. 2018;8(4):114. https://doi.org/10.3390/geosciences8040114
8. Nanditha J, Kushwaha AP, Singh R, Malik I, Solanki H, Chuphal DS. The Pakistan flood of August 2022: causes and implications. Earth's Future. 2023;11(3):e2022EF003230. https://doi.org/10.1029/2022EF003230
9. Ahmad I, Tang D, Wang T, Wang M, Wagan B. Precipitation Trends over Time Using Mann-Kendall and Spearman's Rho Tests in Swat River Basin, Pakistan. Adv Meteorol. 2015;2015(1):431860.
10. Bibi T, Nawaz F, Abdul Rahman A, Azahari Razak K, Latif A. Flood risk assessment of river kabul and swat catchment area: district charsadda, Pakistan. Int Arch Photogramm Remote Sens Spatial Inf Sci. 2018;XLII-4/W9:105–13. https://doi.org/10.5194/isprs-archives-xlii-4-w9-105-2018
11. Bacha MS, Nafees M, Adnan S. Farmers' perceptions about climate change vulnerabilities and their adaptation measures in District Swat. 2018.
12. Archer D. Contrasting hydrological regimes in the upper Indus Basin. J Hydrol. 2003;274(1–4):198–210. https://doi.org/10.1016/s0022-1694(02)00414-6
13. Tran T-N-D, Lakshmi V. Enhancing human resilience against climate change: Assessment of hydroclimatic extremes and sea level rise impacts on the Eastern Shore of Virginia, United States. Sci Total Environ. 2024;947:174289. https://doi.org/10.1016/j.scitotenv.2024.174289 PMID: 38944311
14. Martinec J. Snowmelt - runoff model for stream flow forecasts. Hydrol Res. 1975;6(3):145–54. https://doi.org/10.2166/nh.1975.0010
15. Garee K, Chen X, Bao A, Wang Y, Meng F. Hydrological Modeling of the Upper Indus Basin: A Case Study from a High-Altitude Glacierized Catchment Hunza. Water. 2017;9(1):17. https://doi.org/10.3390/w9010017
16. Zhou G, Cui M, Wan J, Zhang S. A Review on Snowmelt Models: Progress and Prospect. Sustainability. 2021;13(20):11485. https://doi.org/10.3390/su132011485
17. Li X, Williams MW. Snowmelt runoff modelling in an arid mountain watershed, Tarim Basin, China. Hydrolog Process. 2008;22(19):3931–40. https://doi.org/10.1002/hyp.7098
18. Wang Y, Wang Y, Wang Y, Li C, Ju Q, Jin J, et al. Applicability of the HBV model to a human-influenced catchment in northern China. Hydrol Res. 2023;54(2):208–19. https://doi.org/10.2166/nh.2023.092

19. Markstrom SL, Regan RS, Hay LE, Viger RJ, Webb RM, Payn RA, et al. PRMS-IV, the precipitation-runoff modeling system, version 4. US Geological Survey; 2015.
20. Devia GK, Ganasri BP, Dwarakish GS. A Review on Hydrological Models. Aquat Proced. 2015;4:1001–7. https://doi.org/10.1016/j.aqpro.2015.02.126
21. Glavan M, Pintar M. Strengths, weaknesses, opportunities and threats of catchment modelling with Soil and Water Assessment Tool (SWAT) model. Water resources management and modeling. 2012;27.
22. DeWalle DR, Rango A. Principles of snow hydrology. Cambridge University Press; 2008.
23. Butt MJ, Bilal M. Application of snowmelt runoff model for water resource management. Hydrolog Process. 2011;25(24):3735–47. https://doi.org/10.1002/hyp.8099
24. Zhang G, Xie H, Yao T, Li H, Duan S. Quantitative water resources assessment of Qinghai Lake basin using Snowmelt Runoff Model (SRM). J Hydrol. 2014;519:976–87. https://doi.org/10.1016/j.jhydrol.2014.08.022
25. Yatagai A, Kamiguchi K, Arakawa O, Hamada A, Yasutomi N, Kitoh A. APHRODITE: Constructing a Long-Term Daily Gridded Precipitation Dataset for Asia Based on a Dense Network of Rain Gauges. Bullet Am Meteorol Soc. 2012;93(9):1401–15. https://doi.org/10.1175/bams-d-11-00122.1
26. Tahir AA, Hakeem SA, Hu T, Hayat H, Yasir M. Simulation of snowmelt-runoff under climate change scenarios in a data-scarce mountain environment. Int J Digit Earth. 2017;12(8):910–30. https://doi.org/10.1080/17538947.2017.1371254
27. Goodarzi MR, Sabaghzadeh M, Niazkar M. Evaluation of Snowmelt Impacts on Flood Flows Based on Remote Sensing Using SRM Model. Water. 2023;15(9):1650. https://doi.org/10.3390/w15091650
28. Aryal A, Tran T-N-D, Kumar B, Lakshmi V. Evaluation of Satellite-Derived Precipitation Products for Streamflow Simulation of a Mountainous Himalayan Watershed: A Study of Myagdi Khola in Kali Gandaki Basin, Nepal. Remote Sens. 2023;15(19):4762. https://doi.org/10.3390/rs15194762
29. Khan A, Idrees MH. The impact of climate change on the Indus basin: challenges and constraints. Water policy in Pakistan: issues and options. Springer; 2023. p. 225–48.
30. Dahri ZH, Ahmad B, Leach JH, Ahmad S. Satellite-based snowcover distribution and associated snowmelt runoff modeling in Swat River Basin of Pakistan. Proc Pak Acade Sci. 2011;48(1):19–32.
31. R.G.I. C. Randolph Glacier Inventory - A Dataset of Global Glacier Outlines, Version 7. NASA National Snow and Ice Data Center Distributed Active Archive Center; 2023.
32. Outline Boundary of Hindu Kush Himalayan (HKH) Region [Internet]. ICIMOD; 2008.
33. Bahadar I, Shafique M, Khan T, Tabassum I, Ali MZ. Flood hazard assessment using hydro-dynamic model and GIS/RS tools: A case study of Babuzai-Kabal tehsil Swat Basin, Pakistan. J Himal Earth Sci. 2015;48(2):129.
34. Dawood M, Rahman A, Mahmood S, Rahman G, Nazir S. Assessing the impact of climatic change on discharge in Swat river basin using fuzzy logic model. Arab J Geosci. 2021;14(18). https://doi.org/10.1007/s12517-021-08219-4
35. Farzana RG, Shaw R. Flood disasters and land use planning in Swat Valley, Eastern Hindu Kush. Land use management in disaster risk reduction: practice and cases from a global perspective. 2017, p. 179–95.
36. Ali W, Hashmi MZ, Jamil A, Rasheed S, Akbar S, Iqbal H. Mid-century change analysis of temperature and precipitation maxima in the Swat River Basin, Pakistan. Front Environ Sci. 2022;10:973759.
37. Zhang Y-X, Liu G-W, Dai C-L, Zou Z-W, Li Q. Simulation and Prediction of Snowmelt Runoff in the Tangwang River Basin Based on the NEX-GDDP-CMIP6 Climate Model. Water. 2024;16(15):2082. https://doi.org/10.3390/w16152082
38. Yang L, Meng X, Zhang X. SRTM DEM and its application advances. Int J Remote Sens. 2011;32(14):3875–96. https://doi.org/10.1080/01431161003786016
39. Minnett PJ. Satellite remote sensing of sea surface temperatures. Encycloped Ocean Sci. Elsevier Ltd. 2003. p. 2552–63.
40. Zhang Z, Moore JC. Mathematical and physical fundamentals of climate change. Elsevier; 2014.
41. Muhammad S, Thapa A. Improved MODIS TERRA/AQUA composite Snow and glacier (RGI6.0) data for High Mountain Asia (2002-2018). Supplement to: Muhammad, S; Thapa, A (2020): An improved Terra-Aqua MODIS snow cover and Randolph Glacier Inventory 60 combined product (MOYDGL06*) for high-mountain Asia between 2002 and 2018 Earth System Science Data, 12(1), 345-356, https://doi.org/105194/essd-12-345-2020: PANGAEA; 2019. https://doi.org/10.1594/PANGAEA.901821
42. Muhammad S, Thapa A. An improved Terra–Aqua MODIS snow cover and Randolph Glacier Inventory 6.0 combined product (MOYDGL06*) for high-mountain Asia between 2002 and 2018. Earth Syst Sci Data. 2020;12(1):345–56. https://doi.org/10.5194/essd-12-345-2020
43. Pfeffer WT, Arendt AA, Bliss A, Bolch T, Cogley JG, Gardner AS, et al. The Randolph Glacier Inventory: a globally complete inventory of glaciers. J Glaciol. 2014;60(221):537–52. https://doi.org/10.3189/2014jog13j176
44. Muhammad S. Improved MODIS TERRA/AQUA composite snow and glacier (RGI6.0) data for high mountain Asia (2019-2021). PANGAEA; 2022.
45. Hall DK, Riggs GA, Salomonson VV, DiGirolamo NE, Bayr KJ. MODIS snow-cover products. Remote Sens Environ. 2002;83(1–2):181–94. https://doi.org/10.1016/s0034-4257(02)00095-0
46. Parajka J, Blöschl G. Validation of MODIS snow cover images over Austria. Hydrol Earth Syst Sci. 2006;10(5):679–89. https://doi.org/10.5194/hess-10-679-2006

47. Gascoin S, Grizonnet M, Bouchet M, et al. Deriving snow cover fraction from MODIS and Sentinel-2 using a spectral unmixing method. Remote Sensing. 2015;7(5):6182–202. https://doi.org/10.3390/rs70506182
48. Gurung DR, et al. Snow-cover mapping and monitoring in the Hindu Kush-Himalayas using MODIS. International Centre for Integrated Mountain Development (ICIMOD). 2011.
49. Kollert A, Mayr A, Dullinger S, Hülber K, Moser D, Lhermitte S, et al. Downscaling MODIS NDSI to Sentinel-2 fractional snow cover by random forest regression. Remote Sens Lett. 2024;15(4):363–72. https://doi.org/10.1080/2150704x.2024.2327084
50. Muhammad S, Thapa A. Daily Terra–Aqua MODIS cloud-free snow and Randolph Glacier Inventory 6.0 combined product (M*D10A1GL06) for high-mountain Asia between 2002 and 2019. Earth Syst Sci Data. 2021;13(2):767–76. https://doi.org/10.5194/essd-13-767-2021
51. Muhammad S. Improved daily MODIS TERRA/AQUA Snow and Randolph Glacier Inventory (RGI6.0) data for High Mountain Asia (2002-2019). PANGAEA; 2020. https://doi.org/10.1594/PANGAEA.918198
52. Tayal Senzeba Ksh, Bhadra A, Bandyopadhyay A. Snowmelt runoff modelling in data scarce Nuranang catchment of eastern Himalayan region. Remote Sens Appl Soc Environ. 2015;1:20–35. https://doi.org/10.1016/j.rsase.2015.06.001
53. Martinec J, Rango A, Roberts R. Snowmelt Runoff Model (SRM) User's Manual. Complete Book; 2008.
54. Vafakhah M, Nouri A, Alavipanah SK. Snowmelt-runoff estimation using radiation SRM model in Taleghan watershed. Environ Earth Sci. 2015;73(3):993–1003. https://doi.org/10.1007/s12665-014-3449-5
55. Abudu S, Cui C I, Saydi M, King JP. Application of snowmelt runoff model (SRM) in mountainous watersheds: A review. Water Sci Eng. 2012;5(2):123–36.
56. Tahir AA, Adamowski JF, Chevallier P, Haq AU, Terzago S. Comparative assessment of spatiotemporal snow cover changes and hydrological behavior of the Gilgit, Astore and Hunza River basins (Hindukush–Karakoram–Himalaya region, Pakistan). Meteorol Atmos Phys. 2016;128(6):793–811. https://doi.org/10.1007/s00703-016-0440-6
57. Gupta C, Kulkarni AV, Taloor AK. Streamflow modeling and contribution of snow and glacier melt runoff in glacierized Upper Indus Basin. Environ Monit Assess. 2021;193(11):761. https://doi.org/10.1007/s10661-021-09537-6 PMID: 34719750
58. Lutz AF, Immerzeel WW, Kraaijenbrink PDA, Shrestha AB, Bierkens MFP. Climate Change Impacts on the Upper Indus Hydrology: Sources, Shifts and Extremes. PLoS One. 2016;11(11):e0165630. https://doi.org/10.1371/journal.pone.0165630 PMID: 27828994
59. Baig S, Sayama T, Yamada M. Quantifying the changes in the runoff and its components across the Upper Indus River Basin under climate change. J Water Clim Change. 2022;13(9):3416–34. https://doi.org/10.2166/wcc.2022.153
60. Immerzeel WW, van Beek LPH, Bierkens MFP. Climate change will affect the Asian water towers. Science. 2010;328(5984):1382–5. https://doi.org/10.1126/science.1183188 PMID: 20538947
61. Verbunt M, Gurtz J, Jasper K, Lang H, Warmerdam P, Zappa M. The hydrological role of snow and glaciers in alpine river basins and their distributed modeling. J Hydrol. 2003;282(1–4):36–55. https://doi.org/10.1016/s0022-1694(03)00251-8
62. Stewart IT, Cayan DR, Dettinger MD. Changes toward Earlier Streamflow Timing across Western North America. J Clim. 2005;18(8):1136–55. https://doi.org/10.1175/jcli3321.1
63. Hayat H, Tahir AA, Wajid S, Abbassi AM, Zubair F, Hashmi Z ur R, et al. Simulation of the meltwater under different climate change scenarios in a poorly gauged snow and glacier-fed Chitral River catchment (Hindukush region). Geocar Int. 2022;37(1):103–19. https://doi.org/10.1080/10106049.2019.1700557
64. Barnett TP, Adam JC, Lettenmaier DP. Potential impacts of a warming climate on water availability in snow-dominated regions. Nature. 2005;438(7066):303–9. https://doi.org/10.1038/nature04141 PMID: 16292301
65. Huss M, Farinotti D, Bauder A, Funk M. Modelling runoff from highly glacierized alpine drainage basins in a changing climate. Hydrol Process. 2008;22(19):3888–902. https://doi.org/10.1002/hyp.7055
66. Rees HG, Collins DN. Regional differences in response of flow in glacier-fed Himalayan rivers to climatic warming. Hydrol Process. 2006;20(10):2157–69. https://doi.org/10.1002/hyp.6209
67. Dahri ZH, Ludwig F, Moors E, Ahmad S, Ahmad B, Ahmad S, et al. Climate change and hydrological regime of the high-altitude Indus basin under extreme climate scenarios. Sci Total Environ. 2021;768:144467. https://doi.org/10.1016/j.scitotenv.2020.144467 PMID: 33454464
68. Ullah MI, Qureshi KS, Rauf A u, Shah LA. Advanced floodplain mapping: HEC-RAS and ArcGIS pro application on Swat River. J Umm Al-Qura Univ Eng Architect. 2024;:1–14.
69. Umar M, Shakir AS. Estimation of snowmelt contribution for Kalam catchment. Pakistan J Eng Appl Sci. 2015.
70. Ragettli S, Pellicciotti F, Immerzeel WW, Miles ES, Petersen L, Heynen M, et al. Unraveling the hydrology of a Himalayan catchment through integration of high resolution in situ data and remote sensing with an advanced simulation model. Adv Water Resourc. 2015;78:94–111. https://doi.org/10.1016/j.advwatres.2015.01.013
71. Fyffe CL, Brock BW, Kirkbride MP, Mair DWF, Arnold NS, Smiraglia C, et al. Do debris-covered glaciers demonstrate distinctive hydrological behaviour compared to clean glaciers? J Hydrol. 2019;570:584–97. https://doi.org/10.1016/j.jhydrol.2018.12.069
72. Panday PK, Thibeault J, Frey KE. Changing temperature and precipitation extremes in the Hindu Kush-Himalayan region: an analysis of CMIP3 and CMIP5 simulations and projections. Intl J Climatol. 2014;35(10):3058–77. https://doi.org/10.1002/joc.4192